HHS Public Access

Author manuscript

Biomaterials. Author manuscript; available in PMC 2019 October 01.

Published in final edited form as:

Biomaterials. 2018 October ; 179: 109–121. doi:10.1016/j.biomaterials.2018.06.038.

Enzymatically Degradable Alginate Hydrogel Systems to Deliver Endothelial Progenitor Cells for Potential Revasculature Applications

Kevin T. Campbell[1], **Roberta S. Stilhano**[1,2], **Eduardo A. Silva**[1]

[1]Department of Biomedical Engineering, University of California Davis, Davis, California, United States of America

[2]Department of Biochemistry, University of Sao Paulo, Sao Paulo, Brazil

Abstract

The objective of this study was to design an injectable biomaterial system that becomes porous *in situ* to deliver and control vascular progenitor cell release. Alginate hydrogels were loaded with outgrowth endothelial cells (OECs) and alginate lyase, an enzyme which cleaves alginate polymer chains. We postulated and confirmed that higher alginate lyase concentrations mediated loss of hydrogel mechanical properties. Hydrogels incorporating 5 and 50 mU/mL of alginate lyase experienced approximately 28% and 57% loss of mass as well as 81% and 91% reduction in storage modulus respectively after a week. Additionally, computational methods and mechanical analysis revealed that hydrogels with alginate lyase significantly increased in mesh size over time. Furthermore, alginate lyase was not found to inhibit OEC proliferation, viability or sprouting potential. Finally, alginate hydrogels incorporating OECs and alginate lyase promoted up to nearly a 10 fold increase in OEC migration *in vitro* than nondegradable hydrogels over the course of a week and increased functional vasculature *in vivo* via a chick chorioallantoic membrane (CAM) assay. Overall, these findings demonstrate that alginate lyase incorporated hydrogels can provide a simple and robust system to promote controlled outward cell migration into native tissue for potential therapeutic revascularization applications.

Keywords

Injectable biomaterial; Cell delivery; Revascularization; Enzymatically degradable hydrogels; Endothelial progenitor cells; Alginate

Introduction

Despite recent advances in the medical field and efforts to delay disease progression, ischemic vascular diseases remain the leading cause of mortality worldwide [1, 2]. A promising strategy for reversing the progression of these diseases involves delivering cell

Corresponding author: Eduardo A. Silva, Department of Biomedical Engineering, 1 Shields Ave., Davis, CA, USA 95616, esilva@ucdavis.edu, Phone: 1-530-754-7107, Fax: 1-530-754-5739 .

Data availability

These data supporting this study are available within the article and supplementary files are available from the authors upon request.

based therapies to stimulate revascularization in ischemic tissue [3–5]. An emerging paradigm for cell therapies involves isolating cells from host tissue, expanding the cells *ex vivo* and infusing them into ischemic tissue [6, 7]. While clinica applications of cellular therapies to promote revascularization have supported the safety of these cells, the therapeutic benefit of these strategies has been inconsistent [8–10]. Indeed, these simple infusions have resulted in poor localization of cells to ischemic tissue and low survival of the transplanted cells [10–12], thus leading to poor contro over cell fate *in vivo.* Alternatively, the use of biomaterial systems to deliver cells have the potential to overcome some of these limitations through providing a well-definec microenvironment to promote cell survival and retention while presenting a template for tissue formation and improving cell viability [2, 13].

A variety of different cell sources have been delivered using biomaterials *in vivo* to promote revascularization [2, 14–20]. In particular, outgrowth endothelial cells (OECs) are a subpopulation of endothelial progenitor cells (EPCs) that are especially suited for promoting vascularization [21]. OECs orchestrate and induce vasculogenesis *in vivo,* maintain a high proliferative capacity and directly incorporate with native vasculature to promote local tissue neovascularization [19, 21–24]. Importantly, OECs have beer isolated from umbilical cord blood or adult peripheral blood as an autologous cell source capable of attenuating undesirable immunological challenges [21]. However, limitations with the ability of transplanted EPCs to incorporate with host tissue still remain a major obstacle for future clinical applications [19, 25, 26].

Here, we propose developing a simple and effective biomaterial system to allow for a depot of OECs *in vivo* that can promote outward cell migration over time into native host tissue. Alginate, a naturally occurring polysaccharide comprised of α-L-guluronic (G-block) and β-D-mannuronic (M-block) residues, was tested as our biomaterial system as it has been extensively validated for the delivery of different cells, including EPCs [14, 17–20, 27]. Typical methods to create porous alginate scaffolds for cell delivery rely on phase inversion [19, 27], solvent casting [28], gas foaming [29] and three-dimensional (3D) printing [30, 31], though many of these techniques do not allow for minimally invasive delivery through injections. Furthermore, additional costly or timeconsuming modifications might be necessary to promote tissue ingrowth and provide control over delivered cells. These strategies include oxidizing alginate to make the polymer susceptible to hydrolysis [32–34], delivering exogenous factors [19] or creating nonhomogeneous biomaterials to facilitate release [35]. An alternative strategy involves loading alginate hydrogels with OECs and alginate lyase, an enzyme which is produced by a wide range of microorganisms including algae that cleaves glycosidic covalent bonds in alginate polymers [36], to promote cell migration. These alginate hydrogels initially encapsulate cells in a stiff nanoporous material that can decrease in strength and increase in porosity *in situ* after injection as the enzyme degrades the alginate polymer. Thus, controlling alginate lyase concentrations in injectable alginate hydrogels could allow for a simple and cost effective strategy to promote cell release through altering the mechanical properties and mesh size of alginate hydrogels.

Therefore, the objective of this study is to determine if incorporating alginate lyase into alginate hydrogels can provide a controllable microenvironment to promote OEC migration

for potential therapeutic revascularization applications. We hypothesize that alginate lyase concentrations can alter alginate hydrogel mechanical properties and consequently facilitate OEC migration and ultimately their ability to participate in revascularization. In this work, we begin by determining how incorporating various enzyme concentrations effects degradation, swelling, storage modulus and the mesh size of alginate hydrogels over the course of three weeks. Then OECs and human microvascular endothelial cells (HMVECs) were cultured in the presence of various alginate lyase concentrations to determine if the enzyme inhibits OECs proliferation, viability and OEC/HMVEC sprouting potential through a 3D sprouting assay. Finally, we determine how incorporated alginate lyase concentrations effect OEC migration from alginate hydrogels and how these delivered cells can participate in new vessel formation and increase perfusion *in vivo* via the chick chorioallantoic membrane (CAM) assay.

Materials and Methods

Hydrogel Formulation

The alginate polymers used in this study were obtained from Novamatrix (FMC), including LF 10/60 alginate containing a higher G-block content (> 60% as specified by the manufacturer) (MW~ 50 kDa). Hydrogels were prepared by dissolving alginate polymer powder in phosphate buffered saline supplemented with calcium and magnesium ions (PBS++; Life Technologies) and sterile filtering (0.22 μm, Thermo Fisher Scientific). Hydrogels were prepared to create a final concentration of 2% (w/v) polymer alginate solution, 8.4 mg/mL of calcium sulfate (Sigma) and alginate lyase (Sigma) at various concentrations (0, 5, 50 and 500 mU/mL) for degradation, swelling, modulus and polystyrene bead release studies. The mixture was then dispensed into plastic molds with approximately 18 mm diameter and 4 ml height and incubated for at least 25 minutes at room temperature. The alginate polymers used for the OEC studies were treated with activated charcoal to further purify the material and coupled with oligopeptides containing Arg-Gly-Asp (RGD) to allow for cell adhesion as previously described [19, 37]. In short, 1 g of alginate was dissolved in 100 ml of deionized water overnight and mixed with 0.5 g of activated charcoal (Sigma) for half an hour. Alginate was then sterile filtered (0.22 μm, Thermo Fisher Scientific) and lyophilized prior to beginning RGD labeling. N-hydroxysulfosuccinimide (sulfo-NHS, Sigma), 1-ethyl-3-(dimethylaminopropyl) carbodiimide (EDC, Sigma) and oligopeptides (GGGGRGDSP, Peptide 2.0) were then added sequentially to alginate redissolved in 2-(N-morpholino) ethanesulfonic acid (MES, Sigma) buffer at pH 6.5. Oligopeptides and alginate uronic acids were kept at a molar ratio of 1:1000 to yield two oligopeptides per alginate polymer (Degree of Substitution = 2.0). The reaction proceeded for 20 hours prior to purifying the alginate via dialysis against decreasing NaCl solutions in deionized water for four days (MWCO 3500, Thermo Fisher Scientific) [19, 20, 37]. RGD coupled alginate was lyophilized and kept at −20°C for long term storage. When needed, RGD alginate was reconstituted with sterile PBS++ to formulate hydrogels with a final concentration of 2% (w/v) polymer alginate solution, 8.4 mg/mL of calcium sulfate, various concentrations of alginate lyase (0, 5 and 50 mU/mL) and 1 million OECs/ml. Then the alginate solution was dispensed between two sterile glass plates with 1-mm spacers height and incubated for at

least 25 minutes at room temperature before being cut with an 8-mm biopsy punch as previously described [2, 38].

Swelling, Degradation and Rheological Characterization of hydrogels

Alginate hydrogels were prepared as described above with 0, 5, 50 and 500 mU/ml of alginate lyase. Alginate hydrogels were transferred to 12-well plates, each hydrogel was topped with 4 ml of PBS++ and incubated at 37°C. At t= 1 hr, 1, 3, 5, 7, 14 and 21 days hydrogels were removed (n = 3–4), representative images were taken and the hydrogels were weighed to obtain the wet weight (W_S). For swelling and degradation studies, hydrogels were then frozen overnight and lyophilized for 48 hours prior to weighing the hydrogels to obtain the dry weight (W_D). Swelling ratio (Q) was determined by the following equation:

$$Q = \frac{\frac{W_S - W_D}{\rho_W} + \frac{W_D}{\rho_P}}{\frac{W_D}{\rho_P}}$$

Here ρ_w is the density of water and ρ_P is the density of polymer (1.6 g/ml). Degradation was determined by the percent of the dry weight of the hydrogels at any time divided by the dry weight of the hydrogels at t= 1 hr. For rheological characterization, the hydrogels were removed and placed between parallel plates (axial force set at 0.01 N) in a rheometer (HR3, TA Instruments). The hydrogels were then strained over a range of 0.001–5% at a frequency of 1 Hz and values of storage modulus (G') were obtained from the linear viscoelastic region. At least a dozen points were used to obtain the average G' value.

Mesh Size Calculations

Mesh size was estimated for the hydrogels using swelling and rheometry data as previously described [38, 39]. The molecular weight between crosslinks (M_c) was determined via the following equation:

$$M_C = C_P RT / G'$$

Where C_P is the polymer concentration, R is the gas constant and T is the measurement temperature. Mesh size (ξ) is then calculated as follows:

$$\xi = Q^{\frac{1}{3}} l \left(\frac{2M_C}{M_r}\right)^{\frac{1}{2}} C_n^{\frac{1}{2}}$$

Where l is the length of the repeating unit (5.15 Å), M_r is the molecular weight of the repeating unit (194 g/mol) and C_n is the characteristic ratio (21.1), which is a measure of chain stiffness. Mesh sizes were obtained using this equation for hydrogels incorporating 0, 5 and 50 mU/ml of alginate lyase at t= 1 hr, 1, 3, 5, 7, 14 and 21 days.

Brownian Dynamic Mesh Size Simulations

Brownian dynamic simulations were used to predict the mesh size distribution of alginate hydrogels with alginate lyase. In order to initiate the simulations, alginate lyase walkers were randomly placed within a cylinder with the same dimensions of the alginate hydrogel. Random kicks (*dx*) were applied to alginate lyase walkers in the x, y and z directions after each timestep *(dt)* based on the following equation:

$$dx = r * \sqrt{2 * \pi * D_{Mesh} * dt}$$

Where r is a random number from a gaussian distribution and D_{Mesh} is the hindered diffusion coefficient when the walker is within the hydrogel defined below [40, 41]:

$$D_{Mesh} = D * \left(\frac{1}{\xi 2} * \left(1 - 2.1044 * \frac{a}{\xi} + 2.089 * \left(\frac{a}{\xi} \right)^3 - 0.948 * \left(\frac{a}{\xi} \right)^5 \right) * (\xi - a)^2 \right)$$

Where D is the diffusion coefficient of alginate lyase in water given by the Stokes-Einstein equation, ξ is the characteristic length between alginate polymers (mesh size) and a is the hydrodynamic radius of alginate lyase predicted from the globular protein's molecular weight (3.145 nm) [36, 42]. The simulated cylinder was then separated into over 10,000 cubic cells and the alginate lyase walkers were allowed to diffuse within or outside the simulated hydrogel depending on their random kicks. In order to determine how alginate lyase concentration effects mesh size, alginate hydrogels with 0, 5 and 50 mU/ml of alginate lyase were placed in PBS++ also containing an equal concentration of enzyme to allow for homogenous degradation of the hydrogels. Then rheometery and swelling data were obtained for these hydrogels to determine how the mesh size changes over five days in a homogeneous alginate lyase solution (data not shown). This data was then linearly extrapolated and applied to the simulations to determine ξ and correspondingly D_{Mesh} at each timestep over the course of five days based on the alginate lyase concentration in each unit cell. All simulations were performed in Java using Eclipse and the cross-sectional area through the middle of the alginate hydrogels were graphed using MATLAB (Mathworks) and reported.

Polystyrene Bead Release

Polystyrene beads were incorporated into alginate hydrogels to further quantify mesh size changes. Fluorescently labeled polystyrene beads (Sigma) with a 2 μm diameter were mixed with alginate dissolved in PBS++ with 0.01% BSA. Then alginate hydrogels prepared as described above containing 0, 5 and 50 mU/ml of alginate lyase were transferred to 12-well plates, topped with 4 ml of PBS++ containing 0.01% BSA and incubated at 37°C. At t= 1 hr, 1, 3, 5, 7, 14 and 21 days one ml from each well was aliquoted to a new 24 well plate and the fluorescence was quantified via a plate reader. Each well was topped with a fresh ml of PBS++ with 0.01% BSA and returned to incubate at 37°C. Following the collection of data for the last time point, a solution of 0.05 M EDTA in PBS++ with 0.01% BSA is topped in lieu of PBS++ with 0.01% BSA to disintegrate the alginate hydrogels and the remaining

polystyrene beads were quantified via the plate reader to determine the percent of initial released.

Cell Culture

OECs used in this study were isolated from human umbilical cord blood obtained from the UC Davis Umbilical Cord Blood Collection Program (UCBCP) as previously described [21, 38]. Human microvascular endothelial cells (HMVECs) were purchased from commercial source (Lonza). OECs were used at P5 and HMVECs at P8 for all experiments. Both OECs and HMVECs were cultured in EGM-2MV (Lonza) containing EBM-2 with 5% fetal bovine serum (FBS), human epidermal growth factor (hEGF), GA-1000 antibiotic, vascular endothelial growth factor (VEGF) A, human fibroblast growth factor-beta (hFGF-β), hydrocortisone, ascorbic acid and insulin-like growth factor-1 (IGF-1) as supplied by the vendor's kit. N media is defined as EGM-2MV without the addition of growth factors.

OEC Transduction with Luciferase and GFP Reporter

OECs were transduced with a lentiviral vector (pCCLc-MNDU3-luciferase-PGK-EGFP-WPRE) that was kindly provided from the UC Davis/CIRM Institute for Regenerative Cures (Prof. Jan Nolta) [43] to allow for ease of detection as previously described with minor modifications [20]. Briefly, OECs were seeded at a density of 5,000 cells/cm^2 and incubated overnight. The following morning OECs were treated with EGM-2MV containing 20 μg/ml of protamine sulfate (Fisher Scientific) and 0.8 μl/ml of viral vector (pCCLc-MNDU3-luciferase-PGK-EGFP-WPRE). For the control OECs, cells received EGM-2MV supplemented with 20 μg/ml of protamine sulfate. The OECs were incubated for 48 hours at 37°C and then washed with warm sterile PBS. Fresh EGM-2MV media was then added to OECs, they were further incubated at 37°C for 24 hours and GFP expression was confirmed via flow cytometry (FACScan cytometer, BD). A minimum of 10,000 events were analyzed to identify fluorescently positive cells above 95% of control cells.

Proliferation and Viability Assay

OECs were seeded at 5,000 and 50,000 cells per well in 96-well tissue culture plates for proliferation and viability assays respectively. All cells were allowed to adhere to the wells for 24 hours in EGM-2MV media. Then 100 μl of EGM-2MV with alginate lyase at various concentrations (0, 5, 50 and 500 mU/mL) were added to the cells and incubated at 37°C. After 2 days, 10 μl of MTT (3-(4,5-Dimethylthiazol-2-yl)-2,5-diphenyltetrazolium bromide) (Sigma) was added to each well and was incubated for an additional 3 hours. The media was then aspirated, 100 μl of isopropanol (Sigma) was added to each well and placed on a shaker for 15 minutes while protected from light with aluminum foil. The total absorbance at 595 nm was quantified via a plate reader (Spectramax®i3; Molecular Devices) and averaged per condition (n = 6). The data was then normalized to the no alginate lyase control (0 mU/ml).

Sprouting Assay

Cytodex 3 microcarrier (MC) beads (GE Healthcare Life Sciences) were seeded with HMVECs or OECs as previously described in detail [21, 44]. In short, 16.8 mg of MC beads were hydrated in Dulbecco's phosphate-buffered saline (DPBS) overnight at room

temperature with gentle agitation and were then sterilized via autoclaving. After cooling, the sterile MC beads were mixed with 1.5 mL of either HMVECs (~2×10^6 P8 cells) or OECs (~2×10^6 P5 cells) in EGM-2MV medium. The solution of beads and cells were transferred to a 15 ml conical tube and incubated at 37°C for 4 hours with gentle agitation applied every 20 minutes by inverting the tube 3–5 times. The HMVEC or OEC seeded MC beads were then transferred to T25 flasks on a rotating shaker (~1 rev/sec) at 37°C with daily media changes until confluent. Then MC beads seeded with OECs or HMVECs were incorporated within fibrin gels [19, 45]. Briefly, MC beads were suspended in EGM-2MV media and mixed with fibrinogen solution (4 mg/mL in 0.9% NaCI; Sigma) containing aprotinin (~60 μg/mL; Sigma). Then 250 μl of this fibrinogen and MC bead solution were aliquoted in 24-well plates. Finally, 200 μl of thrombin (2.1 U/mL in DPBS; Sigma) was additionally aliquoted into the 24 well plates and the final solution in each well was mixed. The plates were allowed to incubate at room temperature for five minutes before being incubated at 37°C for 25 minutes. For characterizing the response of OEC and HMVEC sprouting in the presence of alginate lyase, 800 μl of EGM-2MV with alginate lyase at various concentrations (0, 5, 50 and 500 mU/mL) were incubated for two days with daily media changes. All gels were then washed with DPBS and fixed overnight at 4°C in 4% formaldehyde. Hoescht 33342 (Life Technologies) was used to stain the cells for fluorescent imaging. The total number of sprouts (n_S) and confluent beads (n_B) were visually quantified per each well. Sprouts were defined as a cell migrating outwards while remaining attached to the bead. The average number of sprouts per bead for each gel, $n_{ave} = n_S/n_B$, was determined and normalized to the no alginate lyase control wells (n = 3). Representative images of sprout formation were taken with an inverted fluorescent microscope (Axio Vert A.4, Zeiss) at 10X magnification.

Migration Assay

The ability of OECs encapsulated within alginate hydrogels incorporating various alginate lyase concentrations to migrate outward from the hydrogels were determined using a migration assay. OECs were encapsulated in hydrogels containing 0, 5 or 50 mU/ml of alginate lyase as described above. OECs encapsulated hydrogels were then placed in 24 well plates, 0.5 ml of EGM-2MV media was added to each well and was incubated at 37°C for one hour to remove any cells on the surface of the hydrogel. Then alginate hydrogels were embedded within fibrin gels by moving the alginate hydrogels to fresh 24 well plates and then adding fibrinogen and thrombin solutions as described above to more closely simulate *in vivo* conditions. The 24 well plates containing alginate/fibrin gels were incubated at 37°C for 30 minutes to ensure full fibrin gelation and 0.8 ml of EGM-2MV media was added to each well. Alginate hydrogels were kept in contact with the fibrin gel and the media was changed daily. At t= 1 hr, 3, 5 and 7 days alginate hydrogels were carefully removed from fibrin gels and were dissolved with trypsin containing 50 mM EDTA at 37°C for five minutes to determine the remaining cells within the hydrogel. The process for removing OECs from fibrin was adapted from previous work [46]. The fibrin was well mixed and trypsin supplemented with 50 mM EDTA was added to the gels for 15 minutes at 37°C to remove migrated cells. The total number of live cells were quantified via trypan blue with a Countess automated cell counter (Life Technologies) and averaged per condition (n = 4–6).

Chick Chorioallantoic Membrane (CAM) Assay

Fertilized hy-line white leghorn chicken eggs (E0) were purchased from the UC Davis Avian Facility and were incubated for three days vertically at controlled temperature and humidity (37.8°C with 90% humidity) with six rotations per day. After 3 days (E3), the eggs were gently cracked open and transferred with aseptic techniques into 88.9 × 88.9 mm weigh boats (Fisher Scientific) in a laminar flow hood. Under aseptic conditions, embryos within the weigh boats were further incubated at 37.8°C with 90% humidity for an additional week. On day 10 (E10), both blank (negative control) and hydrogels disks with OECs and various concentrations of alginate lyase (either 0, 5 or 50 mU/ml) were placed on the CAM avoiding major blood vessels and left on the CAM for three days. Hydrogels were kept hydrated by adding 100 μl of N media to each hydrogel twice a day. Pictures were taken with a 16-megapixel camera (Galaxy Note 4; Samsung Inc.) around the region of the hydrogel location at 0, 24 and 72 hours of incubation ($n = 3–5$). The angiogenic effects were quantified by manually assessing the number of blood vessels between 8 to 10 mm from the center of the hydrogel as previously described [38, 44, 47]. Additionally, at 0, 24 and 72 hours of incubation, blood flow measurements were quantified surrounding the blank and OEC incorporating hydrogels using Periscan system blood perfusion monitor laser Doppler equipment (Perimed, Stockholm, Sweden). The percent change in the number of blood vessels and perfusion over 24 and 72 hours was calculated for each CAM and was normalized to blank controls. Each condition then had the percent difference from the blank control reported. The details of the CAM assay used in this work was officially informed and consulted with the UC Davis Institutional Animal Care and Use Committee (IACUC) Office, however the CAM assay is UC Davis IACUC exempt. UC Davis is an Office of Laboratory Animal Welfare (OLAW), National Institutes of Health (NIH), Public Health Service (PHS) assured institution (UC Davis Animal Welfare Assurance number is #A3433–01) and follows PHS guidance of the definition for what constitutes a live, vertebrate animal.

Statistical Analysis

A one-way analysis of variance (ANOVA) followed by Tukey's test for multiple comparisons was used to assess differences between proliferation, viability and sprouting of cells to varying alginate lyase concentrations. A two-tailed paired Student's t-test was used for the *in vivo* CAM assay to determine if OEC hydrogel conditions led to an increase in vasculature density or perfusion. Differences between experimental conditions for the CAM assay were also compared via a two-tailed unpaired Student's t-test with an applied Bonferroni correction to assess increases in vascular or perfusion between groups. In all cases, significance was asserted at $P < 0.05$. GraphPad Prism software (GraphPad Software Inc.) was used to perform all analyses.

Results

The Mechanical Properties of Alginate Hydrogels Depend on Alginate Lyase Concentrations

The change in mechanical properties of alginate hydrogels with varying concentrations of alginate lyase were assessed over time (Fig. 1A). Alginate hydrogels with 5 mU/ml of alginate lyase were observed to form visible pores, while alginate hydrogels with 50 mU/ml

of alginate lyase showed a noticeable decrease in size after one week (Fig. 1B). Quantifying this degradation determined that hydrogels with 0, 5, 50 and 500 mU/ml of alginate lyase had approximately 83%, 72%, 43% and 0% remaining dry mass respectively after one week (Fig. 1C). Hydrogels with 500 mU/ml of alginate lyase experienced an abrupt and rapid degradation, thus leading to this condition being discontinued from further studies. Interestingly, swelling was initially found to increase with alginate lyase concentrations, though hydrogels with 5 and 50 mU/ml of alginate lyase approached a similar swelling ratio as hydrogels with no alginate lyase after three weeks (Fig. 1D). Storage modulus was also responsive to alginate lyase concentrations, with higher concentrations of alginate lyase leading to both a more rapid loss of strength and an overall lower storage modulus after three weeks (Fig. 1E).

Alginate Mesh Size Increases with Alginate Lyase Concentrations

The change in mesh size of alginate hydrogels with alginate lyase was predicted and quantified using different technical approaches. Computational work applying Brownian dynamics simulations were used to predict the mesh size distributions of alginate hydrogels. These simulations found that alginate hydrogel mesh size varied from approximately 36 nm to 65 nm and 41 nm to 129 nm for hydrogels with 5 and 50 mU/ml of alginate lyase respectively after five days (Fig. 2A). Additionally, the simulations predicted that the mesh size was consistently higher near the center of the hydrogel than the peripherals. Similarly, mesh sizes determined from the swelling and modulus data found that the mesh size of alginate hydrogels was very dependent on alginate lyase concentrations, with hydrogels incorporating 0, 5 and 50 mU/ml of alginate lyase having a mesh size of approximately 40 nm, 78 nm and 98 nm respectively after five days (Fig. 2B). Polystyrene beads were incorporated into alginate hydrogels to provide an indirect determination of mesh size. These polystyrene beads were also found to have an accelerated release from alginate hydrogels containing alginate lyase, with hydrogels incorporating 5 and 50 mU/ml of alginate lyase having approximately 1.2 and 4.4 fold more bead release respectively than the no alginate lyase hydrogels after three weeks (Fig. 2C).

Effect of Alginate Lyase on Endothelial Cell Proliferation, Viability and Sprouting

In order to determine the response of OECs and HMVECs to alginate lyase, cells were cultured with varying concentrations of alginate lyase for proliferation, viability and 3D sprouting assays. OECs were exposed to media supplemented with 0, 5, 50 or 500 mU/ml of alginate lyase for two days and all groups were normalized to the no alginate lyase control. OECs exposed to different concentrations of alginate lyase experienced no significant difference in proliferation after 48 hours (Fig. 3A). Viability of OECs were also found to be independent on lower alginate lyase concentrations, though OECs cultured in the presence of 500 mU/ml of alginate lyase were found to lead to approximately a 22% reduction in viability (Fig. 3B). The effects of alginate lyase on the early stages of blood vessel formation was determined via a 3D sprouting assay (Fig. 3C). HMVECs were used to model the microvasculature found in native tissue. The various concentrations of alginate lyase were not found to lead to any differences in the total number of sprouts for OECs (Fig. 3D) or HMVECs (Fig. 3E).

Alginate Lyase Promotes OEC Migration from Alginate Hydrogels

The ability for OECs to migrate outward from alginate hydrogels with various concentrations of alginate lyase were assessed via a migration assay. Alginate hydrogels containing OECs and varying concentrations of alginate lyase were embedded within fibrin gels to mimic placement in tissue. OECs were found to localize around the alginate hydrogel and fibrin interface without alginate lyase, though hydrogels with both 5 and 50 mU/ml of alginate lyase were observed to have OEC migration from the alginate hydrogels (Fig. 4A). Quantifying OEC migration found that higher concentrations of alginate lyase led to significantly more migration, with approximately 6%, 28% and 66% of the initial alginate encapsulated OECs occupying the fibrin gel after seven days for hydrogels with 0, 5 and 50 mU/ml of alginate lyase respectively (Fig. 4B). The amount of viable OECs populating alginate hydrogels were also found to decrease with higher alginate lyase concentrations, with approximately 89%, 78% and 14% of the initially encapsulated OECs remaining in the alginate hydrogels after seven days for hydrogels with 0, 5 and 50 mU/ml of alginate lyase respectively (Fig. 4C).

Alginate Hydrogels Incorporating Alginate Lyase Promotes New Vasculature in a CAM Assay

The proangiogenic potential of hydrogels with OECs and various concentrations of alginate lyase were assessed *in vivo* via a CAM assay. Alginate hydrogels with OECs and 0, 5 or 50 mU/ml of alginate lyase were placed on separate CAMs with a blank hydrogel to assess changes in vasculature over the course of three days (Fig. 5A). Hydrogels with 5 and 50 mU/ml had a significant increase in new vasculature after one day, leading to approximately 24% and 9% increase in new vessels respectively when compared to the blank control (Fig. 5B). However, after three days only hydrogels with 0 and 5 mU/ml had a significant increase in vasculature, with approximately 4% and 55% increase in new vessels respectively when compared to the blank control. Interestingly, hydrogels with alginate lyase were observed to visibly decrease in size of the course of three days.

Alginate Hydrogels with Low Alginate Lyase Increases Localized Perfusion in a CAM Assay

Finally, the ability of alginate hydrogels with OECs and alginate lyase to increase perfusion in CAMs were assessed with laser Doppler perfusion imaging (LDPI). Alginate hydrogels incorporating OECs and different concentrations of alginate lyase (0, 5 or 50 mU/ml) were placed on separate CAMs with a blank hydrogel to assess changes in perfusion over the course of three days (Fig. 6A). Alginate hydrogels with OECs and either 0 or 50 mU/ml of alginate lyase resulted in no significant increase in perfusion at one or three days when compared to the blank control. In contrast, hydrogels with OECs and 5 mU/ml of alginate lyase led to approximately 2.6 and 5.0 fold increase in perfusion at one and three days respectively when compared to the blank control (Fig. 6B). Interestingly, this increase in perfusion followed a similar trend to the increase in vessel density for the tested alginate hydrogels.

Discussion

This study investigates the utility of an injectable and enzymatically degradable alginate hydrogel system for the delivery of OECs. This work demonstrates that increasing the alginate lyase concentration in alginate hydrogels decreased the mechanical properties and enhanced outward cell migration. Additionally, OECs delivered from these alginate lyase incorporated hydrogels were able to participate in new vessel formation and increase localized perfusion *in vivo* via a CAM assay. To our knowledge, this is the first study characterizing an alginate hydrogel system utilizing alginate lyase to promote cell release for potential therapeutic angiogenic applications.

This work indicates how an enzymatically degradable biomaterial system can be utilized to create adjustable microenvironments for potential revascularization applications. Enzymatically mediated biomaterial degradation has many advantages for regenerative and tissue engineering applications, including creating space for tissue ingrowth and altering local properties to influence cell behavior [48–50]. This has led to the application of many proteolytically degradable biomaterials, including alginate, to allow for cell mediated degradation [51–53]. However, an alternative strategy involves incorporating alginate lyase in alginate hydrogels to facilitate enzymatic degradation. Alginate lyase does not require post-polymerization modifications to exert its enzymatic activity, is not expressed in mammalian cells and degrades alginate hydrogels crosslinked with calcium [54, 55], thus allowing for a method to easily alter alginate hydrogel properties via controlling the concentration of alginate lyase. Previous work delivering neural progenitor cells in alginate hydrogels containing poly(lactide-co-glycolide) (PLGA) microspheres incorporating alginate lyase found that hydrogel degradation was dependent on the concentration of the enzyme [54]. More recent work incorporated alginate lyase into alginate microbeads via electrostatic interactions for bone regeneration applications and also observed accelerated degradation in the presence of higher alginate lyase concentrations [56]. In this study, we apply a widely tested and validated alginate hydrogel system [27, 32, 35, 57–59] to bypass microbead/sphere formation for potential revascularization applications. Our results found that alginate hydrogels experienced significant degradation, increased short term swelling and loss of storage modulus with higher concentrations of alginate lyase over three weeks.

The use of porous biomaterials for cell delivery applications hold great potential for therapeutic strategies due to their ability to mimic natural extracellular matrix and allow cells to migrate, proliferate and function [60]. However, many of these porous forming methods typically require additional processing steps that can be harsh to protein and cell based therapies and do not allow for delivery via injection [61]. In this study, we investigate how initially nanoporous alginate hydrogels increase in porosity in response to encapsulated alginate lyase. Alginate lyase produced from *Azotobacter vinelandii* produces a family of alginate lyase enzymes that are predicted to have a hydrodynamic radius of approximately 3.14 nm based on its molecular weight (50 kDa) [36, 42] and do not always tightly bind to alginate but instead are able to diffuse and relocate [62]. Thus, we applied Brownian dynamic simulations to predict the alginate lyase and mesh size distributions within alginate hydrogels. These simulations found that alginate lyase maintained the highest concentration, and thus a greater mesh size, within the center of the hydrogel after five days. Mesh size

determined using the storage modulus and swelling data also found a similar increasing trend in mesh size for hydrogels incorporating higher enzyme concentrations over the course of three weeks, though the maximum mesh size was only approximately 214 nm and still smaller than the size of a typical endothelial cell. Interestingly, 2 μm polystyrene beads experienced a much faster release from alginate hydrogels than mesh size alone would predict, suggesting that degradation and decrease in hydrogel strength also has a significant role in the observed release. These enzymatically degradable alginate hydrogels were found to increase in mesh size and alter mechanical properties for potential cell release applications.

This study demonstrates that low concentrations of alginate lyase did not inhibit *in vitro* OEC proliferation, viability or OEC/HMVEC sprouting potential. Our results showed that OECs cultured in the presence of 0 to 500 mU/ml of alginate lyase experienced no decrease in proliferation after 48 hours. However, OECs in the presence of 500 mU/ml were found to have a slight, yet significant, decrease in viability. The effect of alginate lyase on the initial stages of blood vessel formation was also tested with a 3D sprouting assay. The 3D sprouting assay is an *in vitro* model that allows for dynamic vessel formation of many different types of ECs throughout an embedded gel to simulate the early events of vessel formation [44, 59, 63, 64]. Various concentrations of alginate lyase between 0 and 500 mU/ml were not found to led to any difference in the number of sprouts for OECs and HMVECs. Previous work has also shown that similar ranges of alginate lyase concentrations did not inhibit neural progenitor cells proliferation *in vitro* [54] or provoke an immune response *in vivo* [56]. Thus, the presence of low concentrations of alginate lyase was not found to have any detrimental effects on OECs or the initial stages of blood vessel formation.

The results from this work also found that higher alginate lyase concentrations induced more OEC migration from alginate hydrogels. Alginate has been utilized to deliver many different cells *in vivo* for cardiovascular applications, including endothelial cells [17, 65], cardiac cells [14], EPCs [19, 20] and stem cells [66, 67], though current techniques to control cell migration and incorporation into native tissue is limited. This has led to studies developing various methods for promoting cell migration from alginate including oxidizing the polymer to be sensitive to hydrolysis [32–34], loading exogenous growth factor to mediate migration [19] or designing the cell carrier to become void forming *in situ* [35]. In this study, we investigated enzymatically degradable alginate hydrogels to promote OEC migration. Hydrogels with 5 and 50 mU/ml of alginate lyase had approximately a 3.6 and 9.7 fold increase in migrated OECs respectively after a week than the hydrogels without alginate lyase. Previous work delivering OECs from oxidized alginate scaffolds was also able to accelerate the release of OECs by approximately 1.0 to 1.5 fold after three days by loading the scaffolds with various isoforms of VEGF [19]. Additionally, we found that hydrogels without alginate lyase experienced very little OEC migration, with only approximately 6% of the cells migrating after a week. This was expected, as these hydrogels maintain a significantly stronger storage modulus and smaller mesh size than hydrogels with alginate lyase thus providing additional polymer sterics and hindering OEC migration. Other work delivering adipose-derived stem cells or mesenchymal stem cells from alginate hydrogels for bone regeneration applications also showed little cell migration for extended periods of time

without designing the hydrogels to degrade or become void forming [35, 56]. Interestingly, higher concentrations of alginate lyase greatly accelerated migration from alginate hydrogels, while lower concentrations of alginate lyase supported cell migration while maintaining a cell depot within the hydrogel after a week. Alginate lyase mediated degradable alginate hydrogels provided a simple and robust method to create a tunable microenvironment to promote OEC migration from alginate hydrogels.

Alginate hydrogels with alginate lyase concentrations stimulated new vasculature *in vivo* via a CAM assay, which is a well-established model for studying angiogenesis and vascular growth [68, 69]. Biomaterial systems have been previously utilized to deliver EPCs to promote vascularization in CAMs [20, 70]. These methods generally utilize relatively weak hydrogels that allow for the delivered cells to displace the material carrier and interact with the CAM to promote new vasculature. In this study, alginate hydrogels with alginate lyase resulted in weaker mechanical properties and increased localized vascularization *in vivo* via a CAM assay. Alginate hydrogels with 5 and 50 mU/ml of alginate lyase had approximately 29% and 9% increase in vasculature respectively after one day, which could be the result of OECs interacting with the CAM microvasculature from the alginate hydrogel through the production of proangiogenic cytokines [27]. However, after three days only the 5 mU/ml condition was significant with approximately a 55% increase in blood vessels. Additionally, alginate hydrogels without alginate lyase did not yield a significant increase in blood vessel after one day, though a slight increase was observed after three days. This is similar to previous work showing that degradable alginate hydrogels could promote more vascularization than nondegradable hydrogels *in vivo* [33]. The lack of significant increases in vascularization in the CAM after three days for hydrogels with 50 mU/ml of alginate lyase could be the result of the limited sensitivity of the migrating OECs to the surrounding CAM microvasculature. Alginate hydrogels with 50 mU/ml of alginate lyase were found to promote migration of OECs at the expense of maintaining OEC retention within the hydrogel. However, the hydrogels were in contact with a two-dimensional monolayer thus limiting OECs in direct contact with the CAM to incorporate with tissue [71–73]. This is in contrast to hydrogels with 5 mU/ml of alginate lyase which promoted both OEC migration and retention *in vitro* and likely supported OECs which could interact with the CAM microvasculature both directly and from the alginate microenvironment through proangiogenic cytokine production [27]. Interestingly, hydrogels incorporating OECs were observed to decrease in size, which was expected as previous work has shown that cells will readily create contractile forces on their surrounding matrix [74–76]. Furthermore, weaker hydrogels support more matrix strains generated from cell-cell communications and allow for the cells to displace polymers, which likely resulted in additional contraction of the hydrogel matrix for hydrogels incorporating alginate lyase [77–81]. Alginate hydrogels with low concentrations of alginate lyase were also found to increase local perfusion. Only alginate hydrogels with 5 mU/ml of alginate lyase led to significant increases in perfusion over three days, with approximately 2.6 and 5.0 fold increase in perfusion at one and three days respectively. Taken together, this work highlights how alginate hydrogels with alginate lyase can deliver OECs in a manner suitable for inducing functional blood vessel formation and thus could have promising revascularization applications.

Conclusions

Biomaterial systems for cell based therapies are a promising strategy for promoting revascularization. In particular, the use of injectable systems to support and promote cell integration with native tissue is attractive for future clinical applications due to their minimally invasive delivery. In this work, the use of enzymatically degradable alginate hydrogels provided a simple method to create controllable microenvironments to induce cell migration which could have future therapeutic applications. This study shows that higher concentrations of alginate lyase mediated loss of hydrogel mechanical properties, increased mesh size and promoted more OEC migration *in vitro.* Furthermore, alginate hydrogels incorporating OECs and low alginate lyase concentrations significantly increased the number of functional blood vessels *in vivo* via a CAM assay. Besides applications for delivering OECs, the therapeutic relevance of utilizing hydrogels incorporating alginate lyase may also benefit other cell based therapies.

Acknowledgements

This work was supported by the American Heart Association (15BGIA25730057 & 17IRG33420114). K.T.C was supported by T32 predoctoral fellowship in basic and translational cardiovascular medicine at UC Davis (T32 HL086350). We thank Dr. Alyssa Panitch and Dr. Kent Leach for the use of equipment involved in acquiring this data. We also thank the UC Davis Umbilical Cord Blood Collection Program (UCBCP) for providing the human umbilical cord blood. We further thank Dr. Jan Nolta and Dr Fernando Fierro for their kind donation of lentivectors.

References

[1]. Ouma GO, Jonas RA, Usman MHU, Mohler ER, Targets and delivery methods for therapeutic angiogenesis in peripheral artery disease, Vascular Medicine 17(3) (2012) 174–192. [PubMed: 22496126]

[2]. Williams PA, Campbell KT, Silva EA, Biomaterials and Cells for Revascularization, in: Emerich DF, Orive G (Eds.), Cell Therapy: Current Status and Future Directions, Springer International Publishing, Cham, 2017, pp. 139–172.

[3]. Copelan EA, Medical progress: Hematopoietic stem-cell transplantation, New Engl J Med 354(17) (2006) 1813–1826. [PubMed: 16641398]

[4]. Couzin J, Vogel G, Cell therapy-Renovating the heart, Science 304(5668) (2004) 192–194. [PubMed: 15073347]

[5]. Srivastava D, Ivey KN, Potential of stem-cell-based therapies for heart disease, Nature 441(7097) (2006) 1097–1099. [PubMed: 16810246]

[6]. Laflamme MA, Murry CE, Heart regeneration, Nature 473(7347) (2011) 326–335. [PubMed: 21593865]

[7]. Losordo DW, Dimmeler S, Therapeutic angiogenesis and vasculogenesis for ischemic disease-Part II: Cell-based therapies, Circulation 109(22) (2004) 2692–2697. [PubMed: 15184293]

[8]. Assmus B, Honold J, Schachinger V, Britten MB, Fischer-Rasokat U, Lehmann R, Teupe C, Pistorius K, Martin H, Abolmaali ND, Tonn T, Dimmeler S, Zeiher AM, Transcoronary transplantation of progenitor cells after myocardial infarction, New Engl J Med 355(12) (2006) 1222–1232. [PubMed: 16990385]

[9]. Lunde K, Solheim S, Aakhus S, Arnesen H, Abdelnoor M, Egeland T, Endresen K, Ilebekk A, Mangschau A, Fjeld JG, Smith HJ, Taraldsrud E, Grogaard HK, Bjornerheim R, Brekke M, Muller C, Hopp E, Ragnarsson A, Brinchmann JE, Forfang K, Intracoronary injection of mononuclear bone marrow cells in acute myocardial infarction, New Engl J Med 355(12) (2006) 1199–1209. [PubMed: 16990383]

[10]. Sanganalmath SK, Bolli R, Cell Therapy for Heart Failure A Comprehensive Overview of Experimental and Clinical Studies, Current Challenges, and Future Directions, Circ Res 113(6) (2013) 810–834. [PubMed: 23989721]

[11]. Hofmann M, Wollert KC, Meyer GP, Menke A, Arseniev L, Hertenstein B, Ganser A, Knapp WH, Drexler H, Monitoring of bone marrow cell homing into the infarcted human myocardium, Circulation 111(17) (2005) 2198–2202. [PubMed: 15851598]

[12]. Rosenzweig A, Cardiac cell therapy-Mixed results from mixed cells, New Engl J Med 355(12) (2006) 1274–1277. [PubMed: 16990391]

[13]. Peppas NA, Hilt JZ, Khademhosseini A, Langer R, Hydrogels in biology and medicine: From molecular principles to bionanotechnology, Advanced Materials 18(11) (2006) 1345–1360.

[14]. Dvir T, Kedem A, Ruvinov E, Levy O, Freeman I, Landa N, Holbova R, Feinberg MS, Dror S, Etzion Y, Leor J, Cohen S, Prevascularization of cardiac patch on the omentum improves its therapeutic outcome, P Natl Acad Sci USA 106(35) (2009) 14990–14995.

[15]. Levenberg S, Huang NF, Lavik E, Rogers AB, Itskovitz-Eldor J, Langer R, Differentiation of human embryonic stem cells on three-dimensional polymer scaffolds, P Natl Acad Sci USA 100(22) (2003) 12741–12746.

[16]. Nor JE, Peters MC, Christensen JB, Sutorik MM, Linn S, Khan MK, Addison CL, Mooney DJ, Polverini PJ, Engineering and characterization of functional human microvessels in immunodeficient mice, Lab Invest 81(4) (2001) 453–463. [PubMed: 11304564]

[17]. Peters MC, Polverini PJ, Mooney DJ, Engineering vascular networks in porous polymer matrices, J Biomed Mater Res 60(4) (2002) 668–78. [PubMed: 11948526]

[18]. Silva EA, Eseonu C, Mooney DJ, Endothelial cells expressing low levels of CD143 (ACE) exhibit enhanced sprouting and potency in relieving tissue ischemia, Angiogenesis 17(3) (2014) 617–630. [PubMed: 24414940]

[19]. Silva EA, Kim ES, Kong HJ, Mooney DJ, Material-based deployment enhances efficacy of endothelial progenitor cells, P Natl Acad Sci USA 105(38) (2008) 14347–14352.

[20]. Torres AL, Bidarra SJ, Pinto MT, Aguiar PC, Silva EA, Barrias CC, Guiding morphogenesis in cell-instructive microgels for therapeutic angiogenesis, Biomaterials 154 (2018) 34–47. [PubMed: 29120817]

[21]. Williams PA, Stilhano RS, To VP, Tran L, Wong K, Silva EA, Hypoxia augments outgrowth endothelial cell (OEC) sprouting and directed migration in response to sphingosine-1-phosphate (S1P), PLoS One 10(4) (2015) e0123437.

[22]. Anderson EM, Kwee BJ, Lewin SA, Raimondo T, Mehta M, Mooney DJ, Local delivery of VEGF and SDF enhances endothelial progenitor cell recruitment and resultant recovery from ischemia, Tissue Eng Part A 21(7–8) (2015) 1217–27. [PubMed: 25434326]

[23]. Melero-Martin JM, De Obaldia ME, Kang SY, Khan ZA, Yuan L, Oettgen P, Bischoff J, Engineering robust and functional vascular networks in vivo with human adult and cord blood-derived progenitor cells, Circ Res 103(2) (2008) 194–202. [PubMed: 18556575]

[24]. Prasain N, Lee MR, Vemula S, Meador JL, Yoshimoto M, Ferkowicz MJ, Fett A, Gupta M, Rapp BM, Saadatzadeh MR, Ginsberg M, Elemento O, Lee Y, Voytik-Harbin SL, Chung HM, Hong KS, Reid E, O'Neill CL, Medina RJ, Stitt AW, Murphy MP, Rafii S, Broxmeyer HE, Yoder MC, Differentiation of human pluripotent stem cells to cells similar to cord-blood endothelial colony-forming cells, Nat Biotechnol 32(11) (2014) 1151–1157. [PubMed: 25306246]

[25]. Krenning G, van Luyn MJA, Harmsen MC, Endothelial progenitor cell-based neovascularization: implications for therapy, Trends Mol Med 15(4) (2009) 180–189. [PubMed: 19303359]

[26]. Tongers J, Losordo DW, Landmesser U, Stem and progenitor cell-based therapy in ischaemic heart disease: promise, uncertainties, and challenges, European Heart Journal 32(10) (2011) 1197–U166. [PubMed: 21362705]

[27]. Vacharathit V, Silva EA, Mooney DJ, Viability and functionality of cells delivered from peptide conjugated scaffolds, Biomaterials 32(15) (2011) 3721–3728. [PubMed: 21334064]

[28]. Radhakrishnan A, Jose GM, Kurup M, PEG-penetrated chitosan-alginate co-polysaccharide-based partially and fully cross-linked hydrogels as ECM mimic for tissue engineering applications, Prog Biomater 4(2–4) (2015) 101–112. [PubMed: 26566468]

[29]. Eiselt P, Yeh J, Latvala RK, Shea LD, Mooney DJ, Porous carriers for biomedical applications based on alginate hydrogels, Biomaterials 21(19) (2000) 1921–1927. [PubMed: 10941913]

[30]. He Y, Yang F, Zhao H, Gao Q, Xia B, Fu J, Research on the printability of hydrogels in 3D bioprinting, Sci Rep 6 (2016) 29977. [PubMed: 27436509]

[31]. Wu Z, Su X, Xu Y, Kong B, Sun W, Mi S, Bioprinting three-dimensional cell-laden tissue constructs with controllable degradation, Sci Rep 6 (2016) 24474. [PubMed: 27091175]

[32]. Bouhadir KH, Lee KY, Alsberg E, Damm KL, Anderson KW, Mooney DJ, Degradation of partially oxidized alginate and its potential application for tissue engineering, Biotechnol Progr 17(5) (2001) 945–950.

[33]. Kong HJ, Kaigler D, Kim K, Mooney DJ, Controlling rigidity and degradation of alginate hydrogels via molecular weight distribution, Biomacromolecules 5(5) (2004) 1720–1727. [PubMed: 15360280]

[34]. Ho SS, Vollmer NL, Refaat MI, Jeon O, Alsberg E, Lee MA, Leach JK, Bone Morphogenetic Protein-2 Promotes Human Mesenchymal Stem Cell Survival and Resultant Bone Formation When Entrapped in Photocrosslinked Alginate Hydrogels, Adv Healthc Mater 5(19) (2016) 2501–2509. [PubMed: 27581621]

[35]. Huebsch N, Lippens E, Lee K, Mehta M, Koshy ST, Darnell MC, Desai RM, Madl CM, Xu M, Zhao XH, Chaudhuri O, Verbeke C, Kim WS, Alim K, Mammoto A, Ingber DE, Duda GN, Mooney DJ, Matrix elasticity of void-forming hydrogels controls transplanted-stem-cell-mediated bone formation, Nature Materials 14(12) (2015) 1269–1277. [PubMed: 26366848]

[36]. Wong TY, Preston LA, Schiller NL, ALGINATE LYASE: review of major sources and enzyme characteristics, structure-function analysis, biological roles, and applications, Annu Rev Microbiol 54 (2000) 289–340. [PubMed: 11018131]

[37]. Rowley JA, Mooney DJ, Alginate type and RGD density control myoblast phenotype, J Biomed Mater Res 60(2) (2002) 217–223. [PubMed: 11857427]

[38]. Williams PA, Campbell KT, Gharaviram H, Madrigal JL, Silva EA, Alginate-Chitosan Hydrogels Provide a Sustained Gradient of Sphingosine-1-Phosphate for Therapeutic Angiogenesis, Annals of Biomedical Engineering 45(4) (2017) 1003–1014. [PubMed: 27904998]

[39]. Madrigal JL, Stilhano RS, Siltanen C, Tanaka K, Rezvani SN, Morgan RP, Revzin A, Han SW, Silva EA, Microfluidic generation of alginate microgels for the controlled delivery of lentivectors, J Mater Chem B 4(43) (2016) 6989–6999.

[40]. Deen WM, Hindered Transport of Large Molecules in Liquid-Filled Pores, Aiche J 33(9) (1987) 1409–1425.

[41]. Khanafer K, Vafai K, The role of porous media in biomedical engineering as related to magnetic resonance imaging and drug delivery, Heat Mass Transfer 42(10) (2006) 939–953.

[42]. Venturoli D, Rippe B, Ficoll and dextran vs. globular proteins as probes for testing glomerular permselectivity: effects of molecular size, shape, charge, and deformability, Am J Physiol-Renal 288(4) (2005) F605–F613.

[43]. Beegle J, Lakatos K, Kalomoiris S, Stewart H, Isseroff RR, Nolta JA, Fierro FA, Hypoxic Preconditioning of Mesenchymal Stromal Cells Induces Metabolic Changes, Enhances Survival, and Promotes Cell Retention In Vivo, Stem Cells 33(6) (2015) 1818–1828. [PubMed: 25702874]

[44]. Campbell KT, Hadley DJ, Kukis DL, Silva EA, Alginate hydrogels allow for bioactive and sustained release of VEGF-C and VEGF-D for lymphangiogenic therapeutic applications, Plos One 12(7) (2017).

[45]. Silva EA, Mooney DJ, Spatiotemporal control of vascular endothelial growth factor delivery from injectable hydrogels enhances angiogenesis, Journal of Thrombosis and Haemostasis 5(3) (2007) 590–598. [PubMed: 17229044]

[46]. Matsumoto T, Sasaki JI, Alsberg E, Egusa H, Yatani H, Sohmura T, Three-Dimensional Cell and Tissue Patterning in a Strained Fibrin Gel System, Plos One 2(11) (2007).

[47]. Williams PA, Campbell KT, Silva EA, Alginate hydrogels of varied molecular weight distribution enable sustained release of sphingosine-1-phosphate and promote angiogenesis, J Biomed Mater Res A 106(1) (2018) 138–146. [PubMed: 28875559]

[48]. Drury JL, Mooney DJ, Hydrogels for tissue engineering: scaffold design variables and applications, Biomaterials 24(24) (2003) 4337–51. [PubMed: 12922147]

[49]. Mann BK, Gobin AS, Tsai AT, Schmedlen RH, West JL, Smooth muscle cell growth in photopolymerized hydrogels with cell adhesive and proteolytically degradable domains: synthetic ECM analogs for tissue engineering, Biomaterials 22(22) (2001) 3045–3051. [PubMed: 11575479]

[50]. Phelps EA, Landazuri N, Thule PM, Taylor WR, Garcia AJ, Bioartificial matrices for therapeutic vascularization, Proc Natl Acad Sci U S A 107(8) (2010) 3323–8. [PubMed: 20080569]

[51]. Fonseca KB, Gomes DB, Lee K, Santos SG, Sousa A, Silva EA, Mooney DJ, Granja PL, Barrias CC, Injectable MMP-Sensitive Alginate Hydrogels as hMSC Delivery Systems, Biomacromolecules 15(1) (2014) 380–390. [PubMed: 24345197]

[52]. Fonseca KB, Maia FR, Cruz FA, Andrade D, Juliano MA, Granja PL, Barrias CC, Enzymatic, physicochemical and biological properties of MMP-sensitive alginate hydrogels, Soft Matter 9(12) (2013) 3283–3292.

[53]. West JL, Hubbell JA, Polymeric biomaterials with degradation sites for proteases involved in cell migration, Macromolecules 32(1) (1999) 241–244.

[54]. Ashton RS, Banerjee A, Punyani S, Schaffer DV, Kane RS, Scaffolds based on degradable alginate hydrogels and poly(lactide-co-glycolide) microspheres for stem cell culture, Biomaterials 28(36) (2007) 5518–5525. [PubMed: 17881048]

[55]. Formo K, Aarstad OA, Skjak-Braek G, Strand BL, Lyase-catalyzed degradation of alginate in the gelled state: effect of gelling ions and lyase specificity, Carbohydr Polym 110 (2014) 100–6. [PubMed: 24906734]

[56]. Leslie SK, Cohen DJ, Sedlaczek J, Pinsker EJ, Boyan BD, Schwartz Z, Controlled release of rat adipose-derived stem cells from alginate microbeads, Biomaterials 34(33) (2013) 8172–8184. [PubMed: 23906513]

[57]. Drury JL, Dennis RG, Mooney DJ, The tensile properties of alginate hydrogels, Biomaterials 25(16) (2004) 3187–3199. [PubMed: 14980414]

[58]. Lee KY, Mooney DJ, Alginate: properties and biomedical applications, Prog Polym Sci 37(1) (2012) 106–126. [PubMed: 22125349]

[59]. Silva EA, Mooney DJ, Effects of VEGF temporal and spatial presentation on angiogenesis, Biomaterials 31(6) (2010) 1235–1241. [PubMed: 19906422]

[60]. Freyman TM, Yannas IV, Gibson LJ, Cellular materials as porous scaffolds for tissue engineering, Prog Mater Sci 46(3–4) (2001) 273–282.

[61]. Loh QL, Choong C, Three-Dimensional Scaffolds for Tissue Engineering Applications: Role of Porosity and Pore Size, Tissue Eng Part B-Re 19(6) (2013) 485–502.

[62]. Hati AG, Aachmann FL, Stokke BT, Skjak-Braek G, Sletmoen M, Energy Landscape of Alginate-Epimerase Interactions Assessed by Optical Tweezers and Atomic Force Microscopy, Plos One 10(10) (2015).

[63]. Nakatsu MN, Sainson RCA, Aoto JN, Taylor KL, Aitkenhead M, Perez-del-Pulgar S, Carpenter PM, Hughes CCW, Angiogenic sprouting and capillary lumen formation modeled by human umbilical vein endothelial cells (HUVEC) in fibrin gels: the role of fibroblasts and Angiopoietin-1, Microvascular Research 66(2) (2003) 102–112. [PubMed: 12935768]

[64]. Schulz MMP, Reisen F, Zgraggen S, Fischer S, Yuen D, Kang GJ, Chen L, Schneider G, Detmar M, Phenotype-based high-content chemical library screening identifies statins as inhibitors of in vivo lymphangiogenesis, P Natl Acad Sci USA 109(40) (2012) E2665–E2674.

[65]. Jay SM, Shepherd BR, Andrejecsk JW, Kyriakides TR, Pober JS, Saltzman WM, Dual delivery of VEGF and MCP-1 to support endothelial cell transplantation for therapeutic vascularization, Biomaterials 31(11) (2010) 3054–3062. [PubMed: 20110124]

[66]. Katare R, Riu F, Rowlinson J, Lewis A, Holden R, Meloni M, Reni C, Wallrapp C, Emanueli C, Madeddu P, Perivascular Delivery of Encapsulated Mesenchymal Stem Cells Improves Postischemic Angiogenesis Via Paracrine Activation of VEGF-A, Arterioscl Throm Vas 33(8) (2013) 1872–1880.

[67]. Man Y, Wang P, Guo YW, Xiang L, Yang Y, Qu YL, Gong P, Deng L, Angiogenic and osteogenic potential of platelet-rich plasma and adipose-derived stem cell laden alginate microspheres, Biomaterials 33(34) (2012) 8802–8811. [PubMed: 22981779]

[68]. Nowak-Sliwinska P, Alitalo K, Allen E, Anisimov A, Aplin AC, Auerbach R, Augustin HG, Bates DO, van Beijnum JR, Bender RHF, Bergers G, Bikfalvi A, Bischoff J, Bock BC, Brooks PC, Bussolino F, Cakir B, Carmeliet P, Castranova D, Cimpean AM, Cleaver O, Coukos G, Davis GE, De Palma M, Dimberg A, Dings RPM, Djonov V, Dudley AC, Dufton NP, Fendt SM, Ferrara N, Fruttiger M, Fukumura D, Ghesquiere B, Gong Y, Griffin RJ, Harris AL, Hughes CCW, Hultgren NW, Iruela-Arispe ML, Irving M, Jain RK, Kalluri R, Kalucka J, Kerbel RS, Kitajewski J, Klaassen I, Kleinmann HK, Koolwijk P, Kuczynski E, Kwak BR, Marien K, Melero-Martin JM, Munn LL, Nicosia RF, Noel A, Nurro J, Olsson AK, Petrova TV, Pietras K, Pili R, Pollard JW, Post MJ, Quax PHA, Rabinovich GA, Raica M, Randi AM, Ribatti D, Ruegg C, Schlingemann RO, Schulte-Merker S, Smith LEH, Song JW, Stacker SA, Stalin J, Stratman AN, Van de Velde M, van Hinsbergh VWM, Vermeulen PB, Waltenberger J, Weinstein BM, Xin H, Yetkin-Arik B, Yla-Herttuala S, Yoder MC, Griffioen AW, Consensus guidelines for the use and interpretation of angiogenesis assays, Angiogenesis (2018).

[69]. Nowak-Sliwinska P, Segura T, Iruela-Arispe ML, The chicken chorioallantoic membrane model in biology, medicine and bioengineering, Angiogenesis 17(4) (2014) 779–804. [PubMed: 25138280]

[70]. Strassburg S, Nienhueser H, Stark GB, Finkenzeller G, Torio-Padron N, Co-culture of adipose-derived stem cells and endothelial cells in fibrin induces angiogenesis and vasculogenesis in a chorioallantoic membrane model, J Tissue Eng Regen M 10(6) (2016) 496–506. [PubMed: 23712963]

[71]. Fuchs A, Lindenbaum ES, The two-and three-dimensional structure of the microcirculation of the chick chorioallantoic membrane, Acta Anat (Basel) 131 (4) (1988) 271–5. [PubMed: 3287831]

[72]. Ribatti D, The chick embryo chorioallantoic membrane (CAM). A multifaceted experimental model, Mech Develop 141 (2016) 70–77.

[73]. Ribatti D, Vacca A, Roncali L, Dammacco F, The chick embryo chorioallantoic membrane as a model for in vivo research on angiogenesis, International Journal of Developmental Biology 40(6) (1996) 1189–1197. [PubMed: 9032025]

[74]. Dembo M, Wang YL, Stresses at the cell-to-substrate interface during locomotion of fibroblasts, Biophysical Journal 76(4) (1999) 2307–2316. [PubMed: 10096925]

[75]. Reinhart-King CA, Dembo M, Hammer DA, Endothelial cell traction forces on RGD-derivatized polyacrylamide substrata, Langmuir 19(5) (2003) 1573–1579.

[76]. Reinhart-King CA, Dembo M, Hammer DA, The dynamics and mechanics of endothelial cell spreading, Biophysical Journal 89(1) (2005) 676–689. [PubMed: 15849250]

[77]. Reinhart-King CA, Dembo M, Hammer DA, Cell-Cell Mechanical Communication through Compliant Substrates, Biophysical Journal 95(12) (2008) 6044–6051. [PubMed: 18775964]

[78]. Reinhart-King CA, How Matrix Properties Control the Self-Assembly and Maintenance of Tissues, Annals of Biomedical Engineering 39(7) (2011) 1849–1856. [PubMed: 21491153]

[79]. Kniazeva E, Weidling JW, Singh R, Botvinick EL, Digman MA, Gratton E, Putnam AJ, Quantification of local matrix deformations and mechanical properties during capillary morphogenesis in 3D, Integr Biol-Uk 4(4) (2012) 431–439.

[80]. Schweller RM, Wu ZJ, Klitzman B, West JL, Stiffness of Protease Sensitive and Cell Adhesive PEG Hydrogels Promotes Neovascularization In Vivo, Annals of Biomedical Engineering 45(6) (2017) 1387–1398. [PubMed: 28361182]

[81]. Discher DE, Janmey P, Wang YL, Tissue cells feel and respond to the stiffness of their substrate, Science 310(5751) (2005) 1139–1143. [PubMed: 16293750]

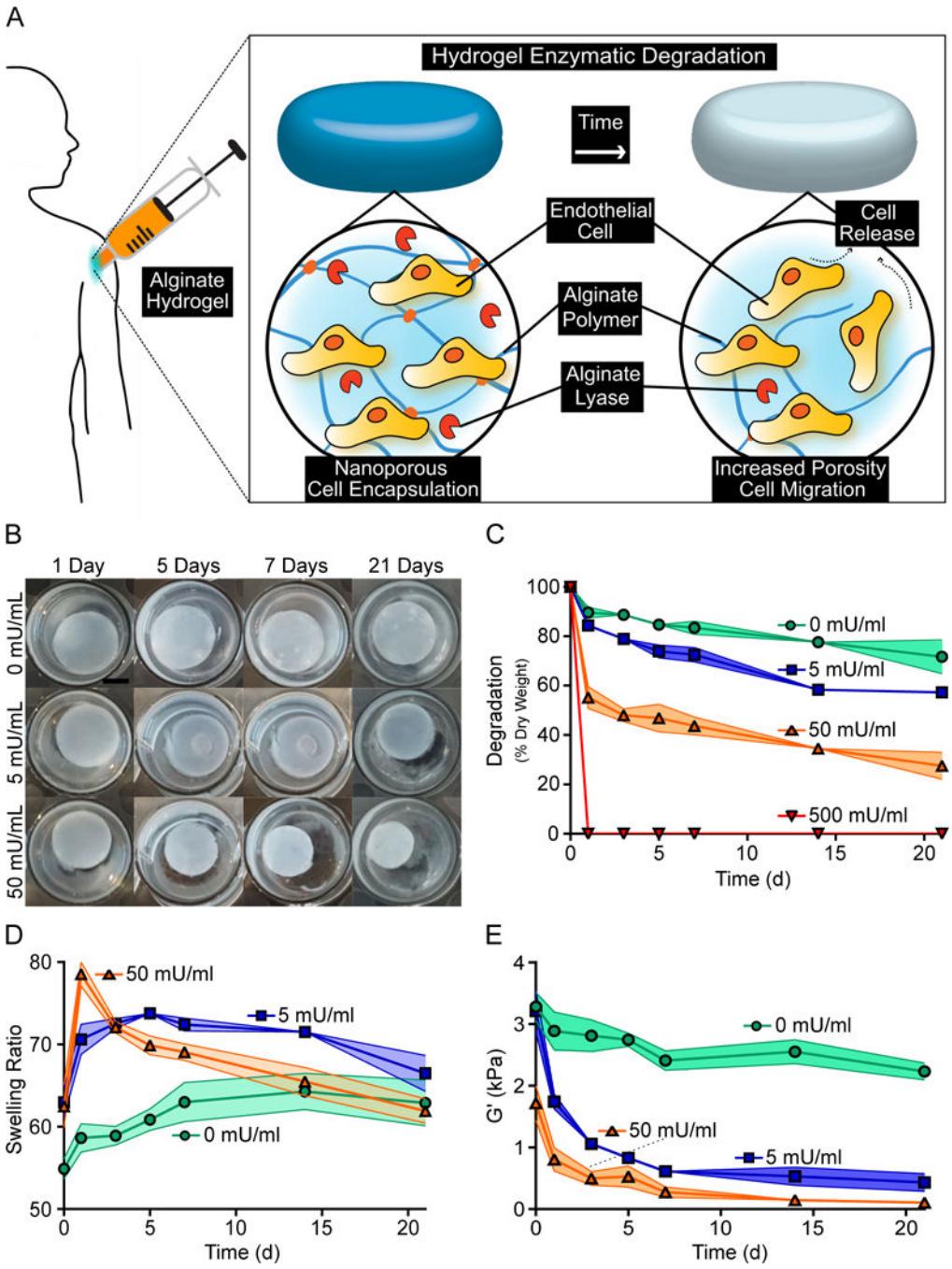

Fig 1. Alginate Hydrogels Experience Decreased Mechanical Properties with Higher Alginate Lyase Concentrations

Alginate hydrogels with higher concentrations of alginate lyase resulted in accelerated degradation and weaker hydrogels over the course of three weeks. A schematic of the proposed cell release mechanism is provided (A). Representative images of hydrogels with various alginate lyase concentration over the course of three weeks are shown. Scale bar represents 5 mm (B). Hydrogels with higher concentrations of alginate lyase experienced greater loss of dry mass (C). Alginate hydrogels had greater short term swelling when incorporating higher concentrations of alginate lyase (D). The Storage modulus abruptly

decreased for hydrogels with alginate lyase (E). Data represent mean ± SD (indicated by shaded areas). (C-E, n = 3–4).

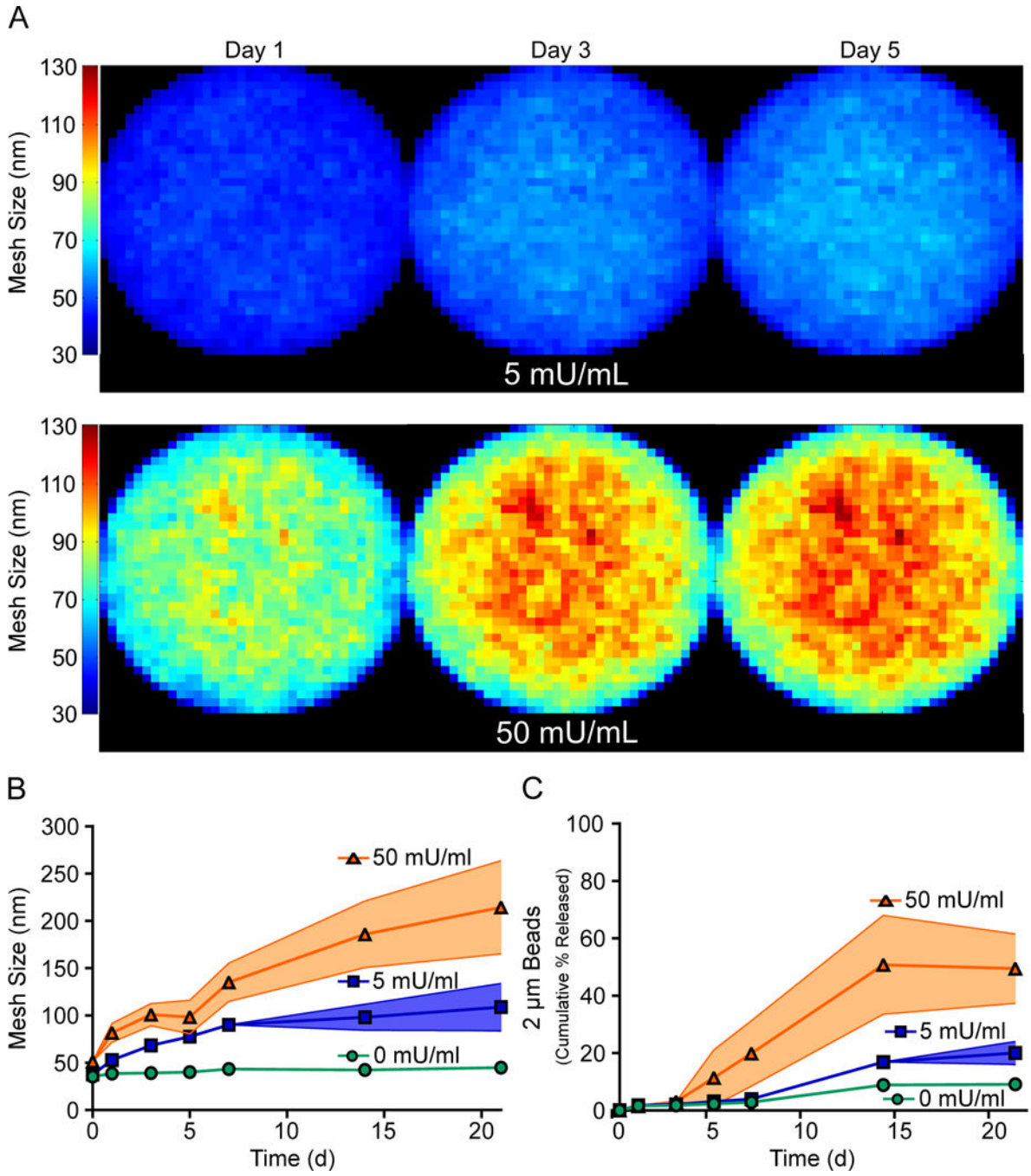

Fig 2. Alginate Lyase Increases the Porosity of Alginate Hydrogels

Alginate hydrogels with higher concentrations of alginate lyase resulted in larger mesh size. Brownian dynamic simulations found that mesh size increased for higher concentrations of alginate lyase, with the greatest increase in mesh size near the center of the hydrogel (A). Mesh size determined from mechanical data also found that the mesh size significantly increases for hydrogels with higher concentrations of alginate lyase (B). Polystyrene beads had faster release from hydrogels incorporating alginate lyase (C). On figure panel A, the

color represents the mesh size of each unit cell of the simulated hydrogel. Data represent mean ± SD (indicated by shaded areas). (B & C, n = 3–4).

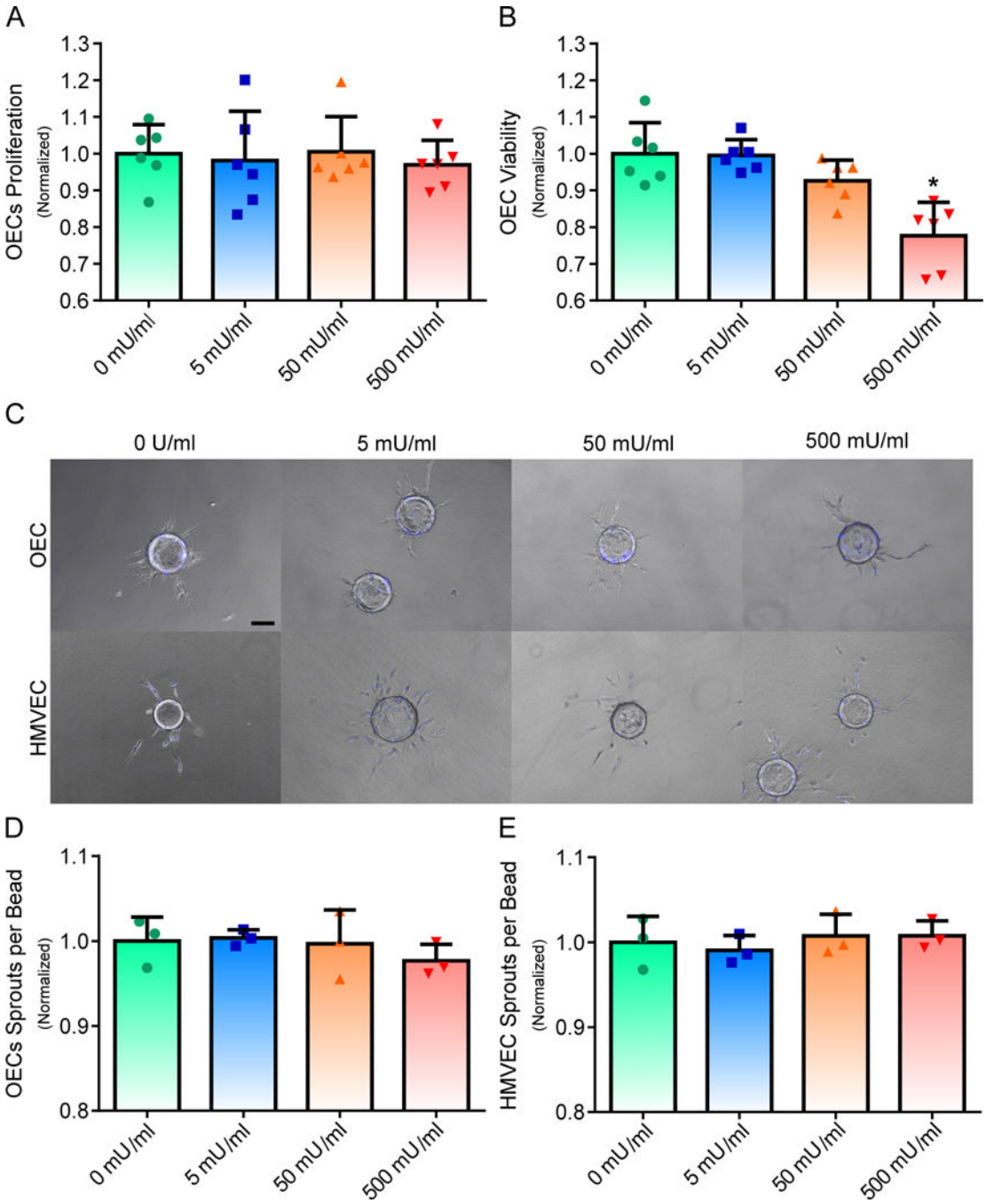

Fig 3. OEC and HMVEC Response is Independent on Low Alginate Lyase Concentrations

Proliferation and viability of OECs were assessed in the presence of various concentrations of alginate lyase (A and B). 3D sprout formation was observed for different concentrations of alginate lyase for OECs and HMVECs. Scale bar represents 100 μm (C). Sprout formation for both OECs and HMVECs were independent on alginate lyase concentrations (D and E). On figure panel A, B, D and E, bar represent mean, scatter dot plots display individual measurements and error bars represent standard deviation. (A & B, n = 6; D & E, n = 3). Asterisk indicate statistically significant differences ($P < 0.05$).

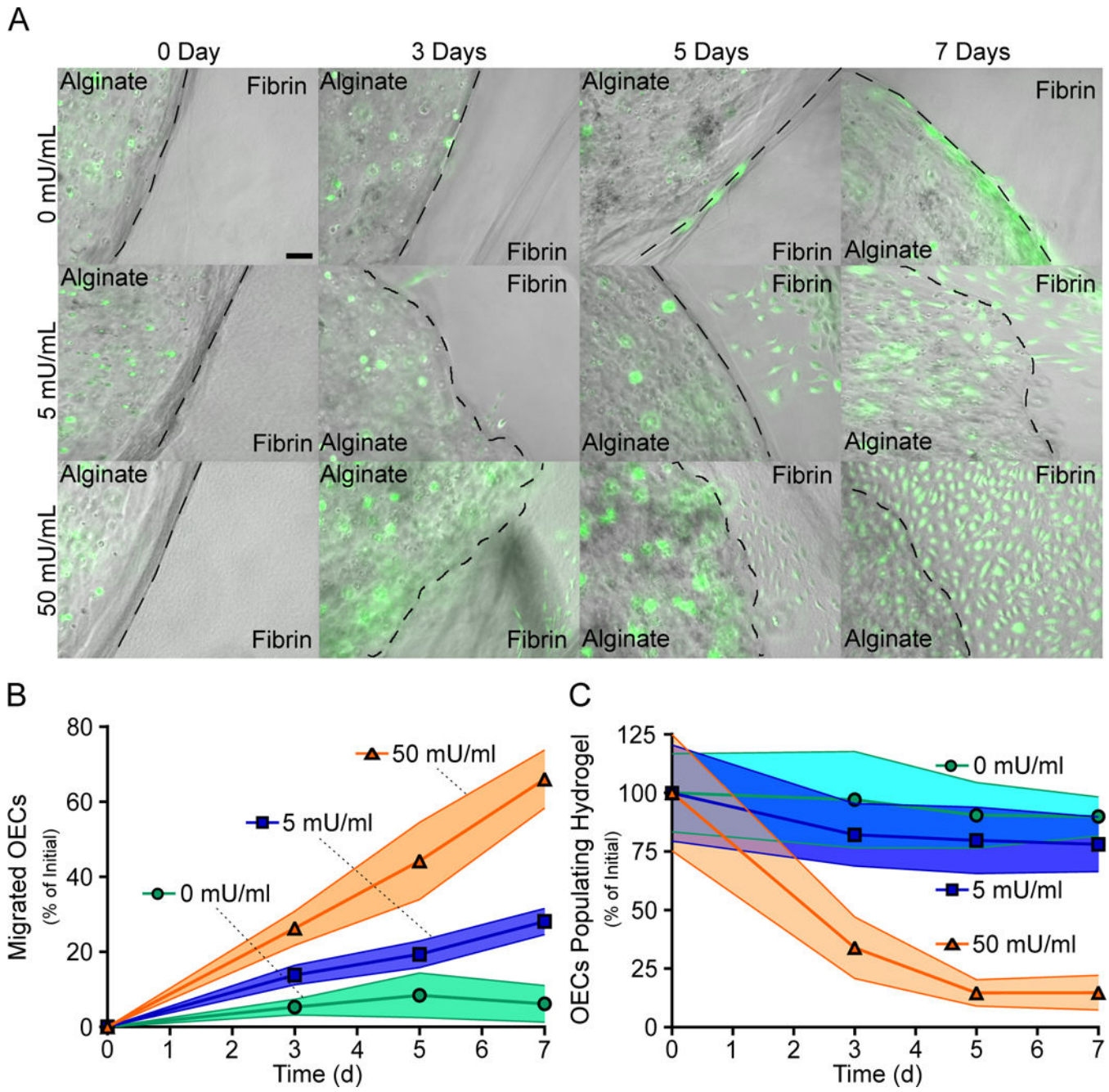

Fig 4. OEC Migration is Accelerated from Hydrogels Incorporating Higher Alginate Lyase Concentrations

OEC migration from alginate hydrogels was found to be dependent on the alginate lyase concentrations. Representative images of the alginate hydrogels embedded within fibrin gels are shown. Scale bar represents 100 μm (A). Quantifying migration found that hydrogels incorporating higher concentrations of alginate lyase promoted significantly faster OECs migration (B). OECs had less retention in alginate hydrogels with higher concentrations of alginate lyase (C). Data represent mean ± SD (indicated by shaded areas). (B & C, n = 4–6).

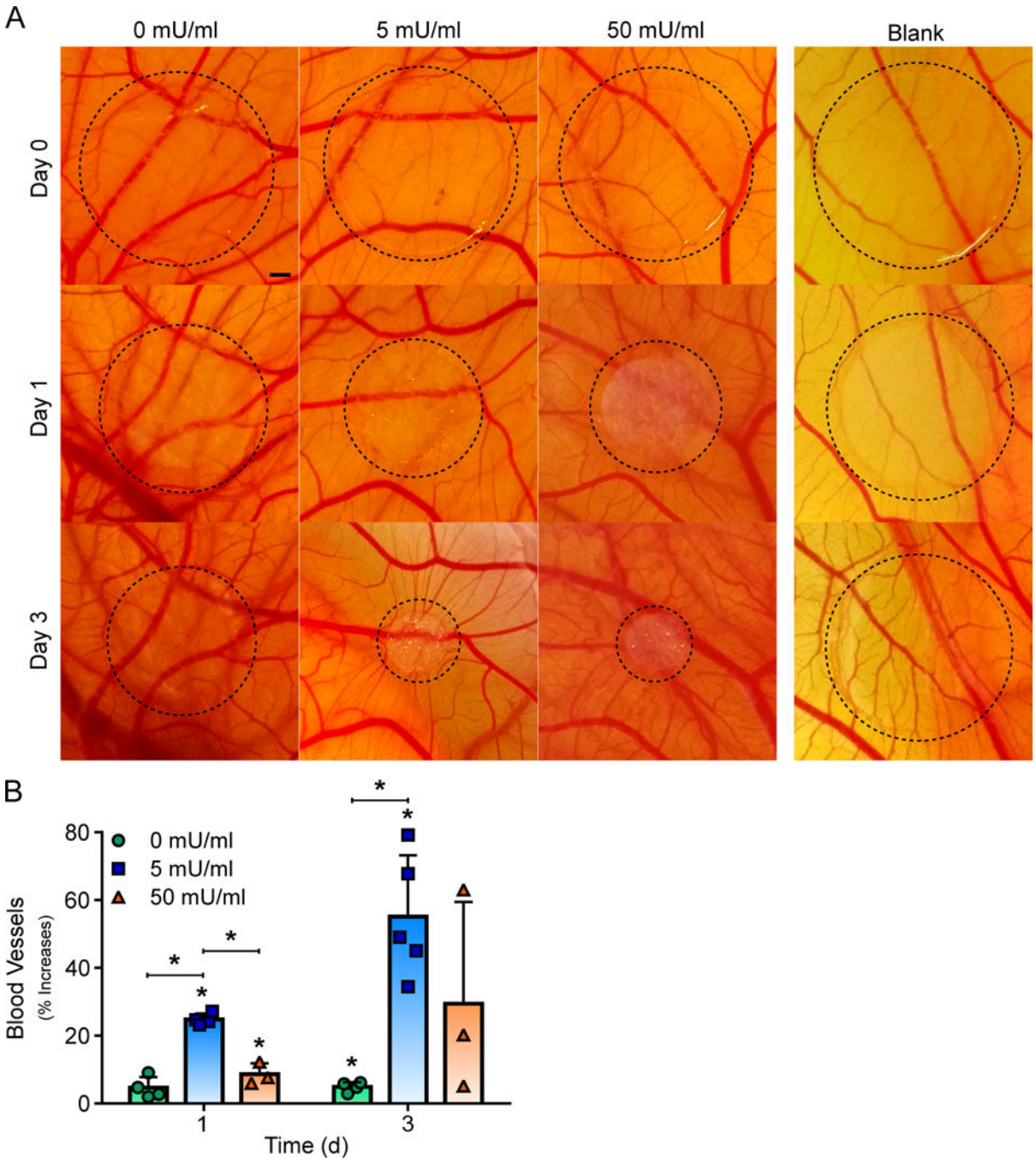

Fig 5. Delivering OECs from Alginate Hydrogels Incorporating Alginate Lyase Enhances Vessel Formation in an *Ex Ovo* CAM assay

Alginate hydrogels with OECs and alginate lyase induced blood vessel formation in a CAM assay. Representative images of the alginate hydrogels with OECs and varying alginate lyase are shown. Scale bar represents 1 mm (A). Quantified blood vessel development showed that alginate hydrogels with OECs and low concentrations of alginate lyase promoted the most significant increase in vascular density (B). On figure panel B, bar represent mean, scatter dot plots display individual measurements and error bars represent standard deviation. (B, n = 3–5). Asterisk indicate statistically significant differences ($P < 0.05$).

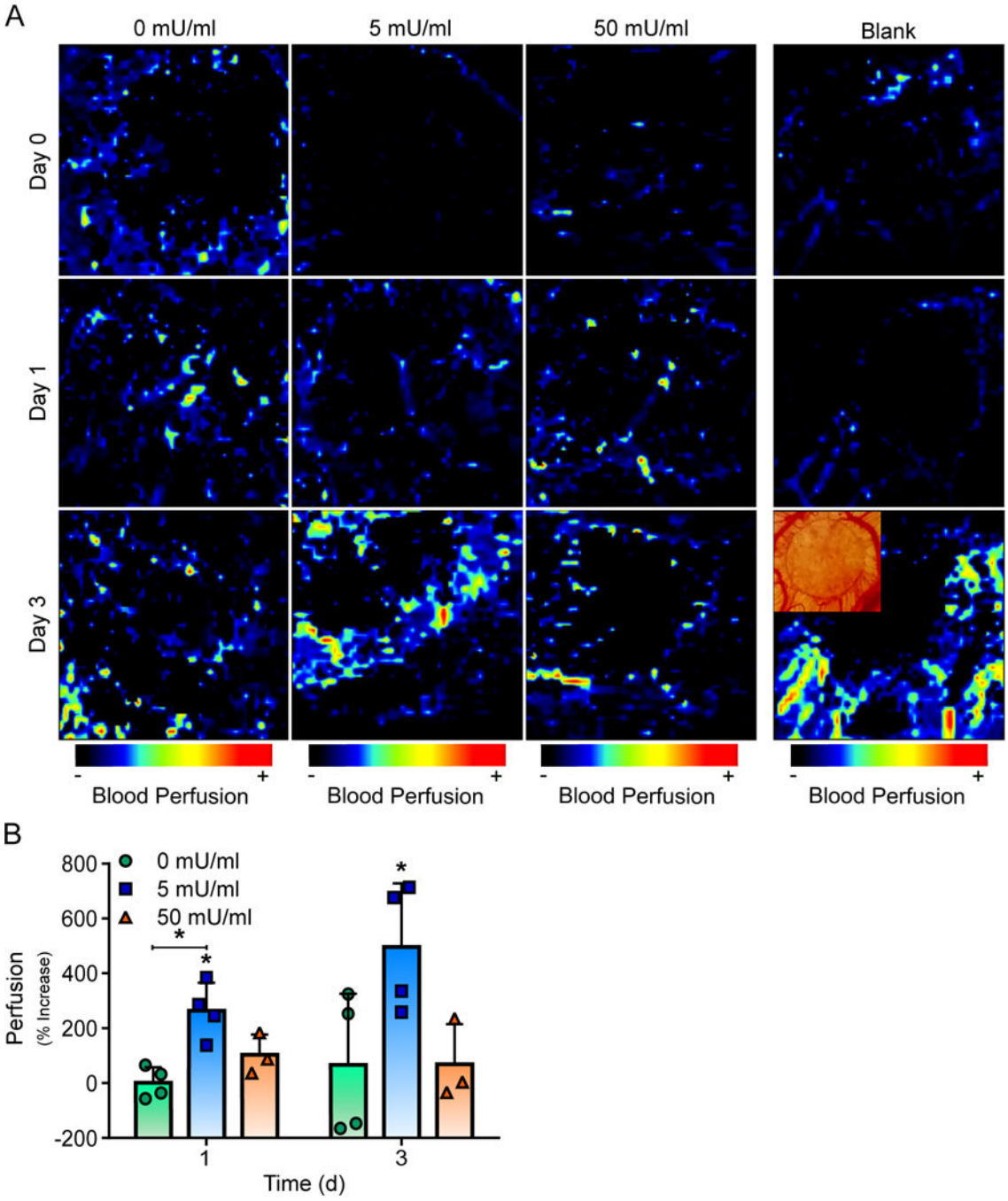

Fig 6. Alginate Hydrogels with OECs and 5 mU/ml of Alginate Lyase Promotes Functional Vasculature in an *Ex Ovo* CAM assay

Alginate hydrogels with OECs and low alginate lyase concentrations promoted increased perfusion in a CAM assay. Representative color coded LDPI images surrounding alginate hydrogels with OECs and varying alginate lyase are shown (A). Quantified perfusion showed that only hydrogels with OECs and 5 mU/ml of alginate lyase promoted significant increases in perfusion (B). On figure panel B, bar represent mean, scatter dot plots display

individual measurements and error bars represent standard deviation. (B, n = 3–4). Asterisk indicate statistically significant differences ($P < 0.05$).